Spray-pyrolyzed Al$_2$O$_3$-Ag Nano-Cerments coatings for solar absorbers

I. Fernández-Peña[a], A. Alvarado-Palacios[a], E. Barrera-Calva[b], J. Calderón-Arenas[a], M. García[c], C. Falcony[d],
R. Fragoso[d], G. Alarcón-Flores[a], C. Paredes-Sánchez[a,e] and M. Aguilar-Frutis[a,*]

[a]*Instituto Politécnico Nacional, Centro de Investigación en Ciencia Aplicada y Tecnología Avanzada,*
Calzada Legaria 694, Col. Irrigación, Del. Miguel Hidalgo, 11500, Ciudad de México, México.
**e-mail: maguilarf@ipn.mx*
[b]*Universidad Autónoma Metropolitana-Iztapalapa, Departamento de Ingeniería de Procesos e Hidráulica,*
Av. San Rafael Atlixco No. 186, Col. Vicentina, Iztapalapa, 09340, Ciudad de México, México.
[c]*Instituto de Investigaciones en Materiales, Universidad Nacional Autónoma de México,*
Circuito Exterior, Ciudad Universitaria, Coyoacán, 04510, Ciudad de México, México.
[d]*Centro de Investigación y de Estudios Avanzados del Instituto Politécnico Nacional,*
Apartado Postal 14-740, 07000, Ciudad de México, 07360, México.
[e]*Escuela Superior de Ingeniería Química e Industrias Extractivas del Instituto Politécnico Nacional,*
Av. Luis Enrique Erro S/N, Unidad Profesional Adolfo López Mateos, Zacatenco, Delegación Gustavo A. Madero, 07738,
Ciudad de México, México.

In this work, it is shown the feasibility for obtaining silver nanoparticles by ultrasonic spray pyrolysis and their simultaneous incorporation during deposition of thin layers of aluminum oxide to get a Cermet coating of Al$_2$O$_3$-Ag. The synthesis of these Cermets was achieved on the basis of both the simultaneous pyrolysis of silver nitrate and aluminum acetylacetonate on different substrates: Quartz, glass, crystalline silicon (c-Si), and titanium at temperatures of 500, 550 and 600°C. The structural properties of the Cermets were studied by Scanning Electron Microscopy, Atomic Force Microscopy and X-ray diffraction. For the optical properties, UV-vis spectroscopy was used to obtain the optical Absorbance of the Cermets, while the Reflectance was obtained by UV-vis-IR spectroscopy measurements. UV-Vis spectroscopy showed that the intensity of the absorption peak (plasmon) was limited to the concentration of silver nitrate, and it shifted toward shorter wavelengths with the decrease in the size of the Ag nanoparticles inside the Cermets. The plasmon position of Ag nanoparticles in the different samples was found to be centered at 504 nm, 506 nm, 497 nm and 475 nm for samples deposited with 0.1 mol, 0.05 mol, 0.02 mol, and 0.01 mol of Ag(NO$_3$), respectively. The shape of the Ag nanoparticles was approximately spherical, ranging from 4 nm to 35 nm, and their concentration was proportional to the concentration of Ag(NO$_3$) included in the spray solution. By means of the UV-Vis Spectroscopy-IR and FT-IR, in the best of cases, a solar absorptance of 0.83 and an infrared thermal emittance of 0.14, for a sample of Al$_2$O$_3$-Ag prepared with 0.1 mol of Ag(NO$_3$) in the precursor solution, were obtained.

Keywords: Al$_2$O$_3$-Ag; nano-cermets; spray pyrolysis; optical properties; structural properties.

PACS: 81.05.Mh; 81.15.Rs; 78.66.Sq

1. Introduction

The research and development of solar collectors or solar energy materials (materials capable of converting solar radiation into thermal energy) has recently increased due to the high demand, which has been directed toward the profitable use of solar energy [1-3]. A category of materials used for this purpose is one that is given by a coating type composed of metal-dielectric material. These types of materials, called Cermets, are systems composed of a ceramic matrix and a metallic component [3,4]. In these materials, the ceramic matrix can be constituted by an insulator metallic oxide or an oxide semiconductor, such as SiO$_2$, Al$_2$O$_3$, Cr$_2$O$_3$, SnO$_2$, etc., while the metal component that has been used can be Cu, Ag, Au, Mo, Co, Ni, Cr, Pt, Fe, Mn, etc., in nanometric dimensions [5-8]. The Cermets can exhibit excellent optical, thermal, and structural properties that make them of particular interest in different applications, apart from the photo-thermal solar energy conversion, such as waveguides, materials with photo-chromic or photo-electrochemical properties and gas

sensors [9-12]. The photo-thermal applications are possible because these materials may show a high solar absorptance (or low reflectance), in the region of $0.3 < \lambda < 3$ μm, combined with a low thermal emittance or low heat transfer (high reflectance in the region $3 < \lambda < 100$ μm) [3]. For applications of such solar collectors, it is necessary that these materials are resistant to high temperatures without degradation of the high selectivity (absorptance/emittance ratio) [4]. Within the techniques developed for the fabrication of different Cermets, there are those that are based on physical or chemical principles such as Sputtering [1,6,13], Dip-Coating [7,14], Evaporation [5,15,16], Anodizing [17,18], among others. However, very rarely the Ultrasonic Spray Pyrolysis (USP) technique has been used to synthesize such materials. The literature reports limited research in the manufacture of photo-thermal materials using the spray pyrolysis technique [19-21]. The USP method has been frequently and successfully used in the past decades; it is considered as a simple, non-expensive technique for depositing thin and

thick films. It could be scalable for industrial applications [19]. The USP method implies the pyrolysis of a spray that has previously been produced by ultrasonic means. The generated mist is then thermally decomposed on top of a surface, which is normally referred as a substrate, leading to the thin or thick solid layer [20]. The USP technique has been used to get a wide variety of materials, mainly metal oxides for different applications [19]. Research in the Al$_2$O$_3$-Ag Cermet, as selective materials to solar radiation, has been carried out very successively on coatings deposited by sputtering [1]. On the other hand, silver has been used as a metal component in various matrices such as SiO$_2$ and in partially oxidized amorphous silicon (a-Si) [6,13,22], whereas aluminum oxide has been the host material for different metal components [4,8,15-18,23,24]. Aluminum oxide (Al$_2$O$_3$) is a very stable material at high temperatures, in addition to the fact of being an excellent diffusion barrier for oxygen, making it a good insulating composite component [4]. Generally, this oxide has an amorphous structure and it has been a remarkable material for different studies, including those related to integrated circuits in MOS devices [25-27]. In the present work, it is shown the feasibility of obtaining Cermet type coatings of Al$_2$O$_3$-Ag deposited by the USP technique. The Cermets of Al$_2$O$_3$-Ag were synthesized on titanium, c-Si, quartz and glass substrates, at temperatures of 500, 550 and 600°C. It was found that the concentration of particles of Ag was dependent on the concentration of Ag(NO$_3$) incorporated in the precursor solution. The shape of the Ag nanoparticles was approximately spherical, and their size was approximately in the range from 4 nm to 35 nm. It was noticed that the position of the plasmon resulted with a shift toward shorter wavelengths with the decrease in the size of the Ag nanoparticles into the Cermets. In the best of cases, a solar selectivity S $\sim$ 6 (S = Absorptance/Emittance), (corresponding to 0.83 absorptance and 0.14 emittance), was obtained in a Cermet of Al$_2$O$_3$-Ag prepared with 0.1 mol of Ag(NO$_3$) and deposited on a not-polished surface of titanium substrate.

2. Materials and Methods

The Cermets of Al$_2$O$_3$-Ag were obtained from silver nitrate (Ag(NO$_3$), Sigma Aldrich), as a source of silver (Ag) and aluminum acetylacetonate (Al(C$_5$H$_7$O$_2$)$_3$ or Al(acac)$_3$, Sigma-Aldrich), as a source of aluminum (Al). Deionized water was used as solvent for Ag(NO$_3$), while N,N-Dimethylformamide (N,N-DMF) was the solvent for Al(acac)$_3$. A 0.1 mol concentration of Al(acac)$_3$ was used for all Cermets, whereas the Ag(NO$_3$) concentration was varied in molarities of 0.01, 0.02, 0.05 and 0.1 Mol. The synthesis was carried out at deposition temperatures of 500, 550 and 600°C on quartz, pyrex glass, c-Si and titanium (Ti) substrates. The titanium substrates were subjected to a cleaning process and most of them were polished, whereas the c-Si, quartz and pyrex glass substrates were only cleaned prior to the deposition of the Cermets. In this work, two ultrasonic humidifiers, operating at a frequency of 800 kHz, were used, each one for the

solutions of Ag(NO$_3$) and Al(acac)$_3$ with their respective solvents. In all cases, air was used as the carrier gas at a flow rate of 10 liters per minute and at a pressure of 40 psi. The deposition time to get the Cermet films was lower than 25 minutes, and their thicknesses were obtained between 200 nm and 850 nm. In the spray pyrolysis technique, the thickness of the film is generally limited to several experimental conditions like the concentration of the chemical precursors, the deposition time and the temperature of synthesis [19,20]. In our case, from the measured values of thicknesses of the films, the deposition rate was about 20 nm/min in average.

The characterization was carried out by means of structural and optical techniques. A scanning electron microscope (SEM) from Jeol, model JSM-6390LV, and a Park Scientific Instruments atomic force microscope were used in the morphological characterization. The elemental composition of the coatings was obtained by Energy Dispersive Specroscopy (EDS). An Inca x-sight Oxford Inst. 7582 model spectrometer, located inside the Jeol SEM, was used for this purpose. The X-ray diffraction (XRD) measurements were performed in a Bruker D8 Advance Diffractometer. The diffraction measurements were acquired in grazing angle condition (incidence angle $\sim 3°$). The optical characterization was carried out in a Cary 5000 and Cary 50 conc spectrophotometers, from Varian, as well as in iS50 FTIR spectrophotometer. The optical absorption was measured in the range from 200 to 1100 nm. For this case, the coatings were deposited on quartz substrates. The computation of the absorptance was performed on the % Reflectance spectra acquired in the range from 200 nm to 2500 nm; for this purpose the coatings were deposited on Titanium substrates. Finally, the emittance was computed from the % Reflectance spectra which were acquired in the range from 2500 nm to 25000 nm; in this case, the coatings were also deposited on Ti substrates. A few Cermets were deposited on c-Si for AFM studies. The thicknesses of the Cermet films were measured in a surface profilometer system from Veeco (model Dektak^3).

3. Results

The pyrolysis of Ag(NO$_3$) and Al(acac)$_3$ has already been suggested in the literature and can be summarized as follows: the decomposition reaction for Al(acac)$_3$, carried out at 400°C, is given by the following chemical reaction:

$$Al(Acac)_3 \xrightarrow{H_2} Al - Oxide + Acetone + Hydrogen - Carbon$$

Where, as a result of the decomposition, aluminum oxide is obtained, as well as byproducts such as acetones and related compounds with hydrogen and carbon. This reaction has been reported by using hydrogen as carrier gas [28]. However, from previous results for synthesizing aluminum oxide, using the USP technique, the reaction takes place from lower temperatures and using air as carrier gas [26]. On the other hand, the thermal decomposition of the Ag(NO$_3$) has been studied at temperatures between 275°C and 575°C. It

has been reported that the decomposition occurs in a single step, producing silver oxide (Ag_2O) without the formation of an intermediate product. In addition to this, the reaction produces NO_2 as the sole product containing nitrogen. The chemical reaction suggested is:

$$4Ag\,NO_3 \rightarrow 2Ag_2O + 4NO_2 + O_2$$
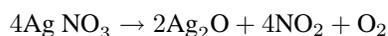
but if the reaction is carried out at a temperature approximately of 550°C, the reduction of the silver oxide to metallic Ag is observed with the loose of O2 according the following chemical equation [21]:

$$Ag_2O \rightarrow 2Ag° + \frac{1}{2}O_2$$
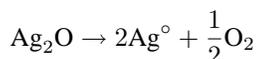
In this way, this previous knowledge about the decomposition of the different reagents was taken into consideration in order to carry out a single and simultaneous reaction, where, in a parallel way; the formation of a solid layer of aluminum oxide, and at the same time, the generation of Ag nanoparticles was achieved in a single solid coating (Al_2O_3-Ag Cermet). The versatility of the USP technique has been used in many works to get systems of thin layers consisting of more than one component, for example thin layers of $CuCrO_2$ [29]. Previous studies have shown the high quality obtained in coatings of aluminum oxide deposited from acetylacetonate of aluminum, using the USP technique at temperatures of 400°C and up to 650°C and with different concentrations of acetylacetonate of aluminum in solutions [25-27]. In this new work, the goal is to show the interesting characteristics of the films that result from the simultaneous pyrolysis of silver nitrate and aluminum acetylacetonate.

The first result is shown in Fig. 1, which shows the XRD diffraction patterns of Al_2O_3-Ag Cermets deposited at 550°C and 600°C on glass substrates and deposited with 0.1 mol of

$Ag(NO_3)$ in the spraying solution. These diffraction pattern show reflections at $2\theta = 38.1°$, 44.3°, 64.5° and 77.5°, corresponding to the (111), (200), (220) and (311) diffraction planes of Ag, respectively (PDF No. 01-087-0720). No reflections are observed for Al_2O_3, suggesting its amorphous structure. This result seems to confirm that the previous reactions are likely to be carried out simultaneously, which favors the synthesis of Al_2O_3-Ag Cermets. In addition to this, it is highlighted the fact that the Cermet is obtained in nanostructured dimension.

SEM and AFM micrographs are shown in Figs. 2a-2e. The SEM micrographs show the surface morphology of the Al_2O_3-Ag Cermets deposited with 0.01, 0.02, 0.05 and 0.1 mol of $Ag(NO_3)$ at a temperature of 600°C on titanium substrates. The SEM micrographs show clearly the Ag particles. An estimate of the size of the Ag particles is done through a histograms analysis, which is displayed next to the SEM micrographs. The AFM micrographs highlight the shape and distribution of the Ag nanoparticles in two selected Cermets.

The histograms represent the size distribution of the Ag particles. A large number of Ag particles ($\sim$100-200) were randomly selected from the SEM images to get the above histograms. The use of the Image J software was also used for this task. The elemental composition of a selected set of coatings was realized by EDS. A silver content of about 10.77 wt% and 21.66 wt% was obtained in samples deposited with 0.02 Mol and 0.1 Mol of $AgNO_3$, respectively (EDS spectra not shown). The AFM micrograph (2e) correspond to a Cermet coating deposited at 500°C on c-Si with a concentration of 0.05 Mol of $AgNO_3$, and to a Cermet coating deposited at 500°C on glass substrate with a concentration of 0.05 mol of $AgNO_3$ (2f).

Figure 3 shows the different optical absorption spectra as a function of wavelength for the coatings that were deposited on quartz at 600°C. These spectra were acquired in Cermets deposited with different contents of $Ag(NO_3)$ in the start solution.

Table I resumes the value of the position of the plasmon peak depicted in Fig. 3, among other results of the main cermets prepared.

A correlation between the position of the plasmon peak and the size of the Ag particles is shown in Fig. 4.

The computation of the solar absorptance (α) was obtained through the equation; $\alpha = 1 - (1/n)\sum_{j=1}^{n} \rho_j$, where ρ_j refers to the reflectance of the Cermets [2]. The absorptance was considered in a region from 200 to 2500 nm in the Cermets deposited on Ti substrates. Similarly, the emittance (ε) was also computed in the range from 2500 nm to 25000 nm, using the following relation; $\varepsilon = 1 - (1/n)\sum_{j=1}^{n} \rho_j$. From the reflectance spectra, the absorptance and emittance were computed and the results are listed in Table I, while the UV-vis-IR and FT-IR spectra are shown in Figs. 5 and 6, respectively.
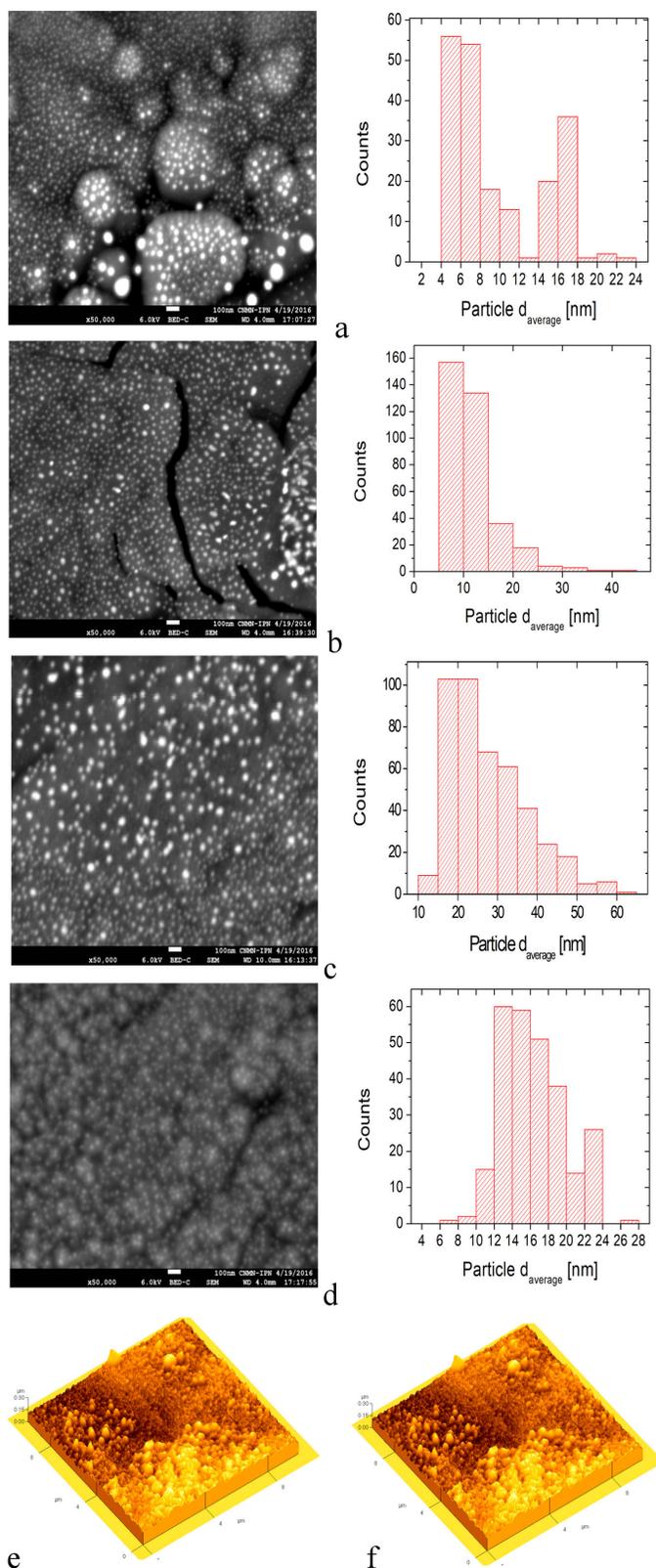

FIGURE 1. Diffraction patterns of Al_2O_3-Ag Cermet coatings deposited at 550°C and at 600°C with 0.1 mol concentration of $AgNO_3$ in initial solution.

FIGURE 2. SEM and AFM micrographs of Al$_2$O$_3$-Ag Cermet coatings. The SEM micrographs correspond to coatings deposited at 550°C on Ti substrates with different concentrations of AgNO$_3$: 0.01 mol (2a), 0.02 mol (2b), 0.05 mol (2c), and 0.1 mol (2d). The histograms represent the size distribution of the Ag particles. The AFM micrograph (2e) correspond to a Cermet coating deposited at 500°C on c-Si with a concentration of 0.05 Mol of AgNO$_3$, and to a Cermet coating deposited at 500°C on glass substrate with a concentration of 0.05 mol of AgNO$_3$ (2f).

TABLE I. Plasmon peak, Absorptance (α) and Emittance (ε) of the Al_2O_3-Ag Cermet coatings obtained by USP at different deposition temperatures on different substrates.

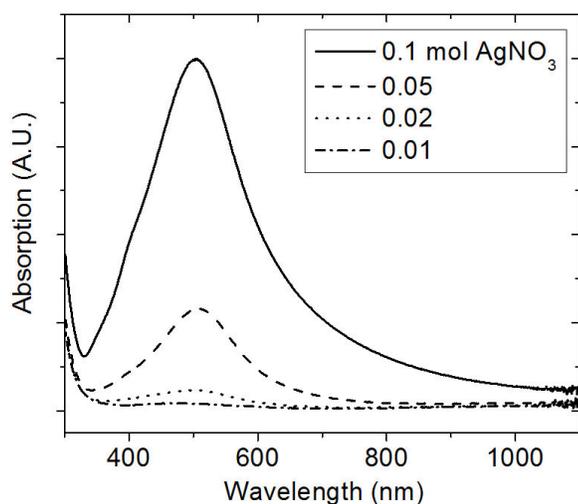| % mol $Ag(NO_3)$	$T_{deposition}$ (°C)/Substrate	Position of absorption peak	Absorptance α	Emittance ε
0.01	600/quartz	475 nm		
0.02	600/quartz	497 nm		
0.05	600/quartz	506 nm		
0.1	600/quartz	504 nm		
0.02	550/polished Ti		0.73	0.43
0.05	550/polished Ti		0.79	0.55
0.1	550/polished Ti		0.78	0.51
0.1	550/not polished Ti		0.83	0.14

FIGURE 3. Optical absorption as a function of wavelength for Al_2O_3-Ag Cermet coatings deposited on quartz at 600°C, and with different concentrations of $AgNO_3$ in precursor solution.

FIGURE 5. % Reflectance spectra for Al_2O_3-Ag Cermet coatings as a function of the wavelength in the solar region of the electromagnetic spectrum.
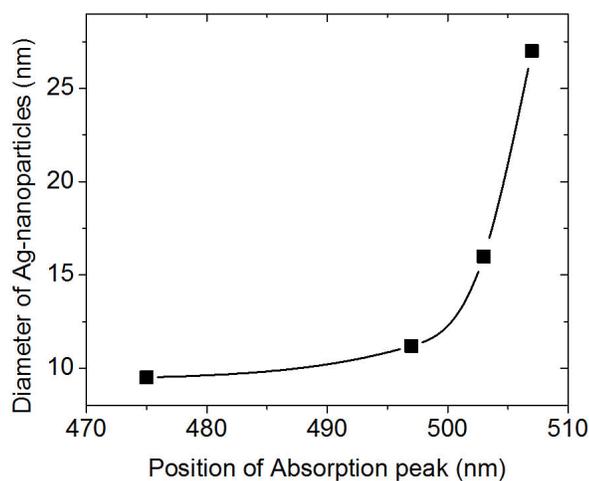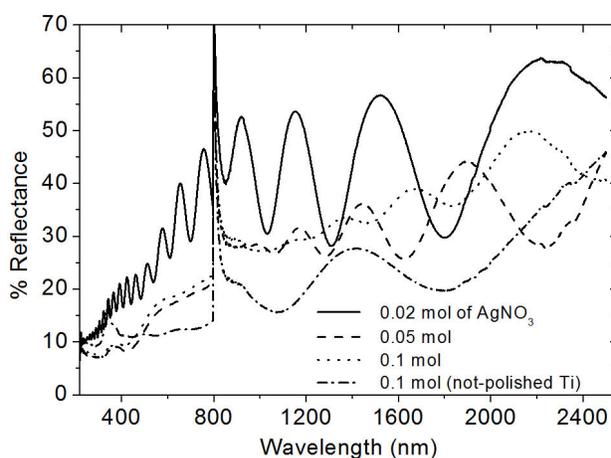

FIGURE 4. Average diameter of the Ag nanoparticles as a function of the maximum absorption peak for Al_2O_3-Ag Cermet coatings.
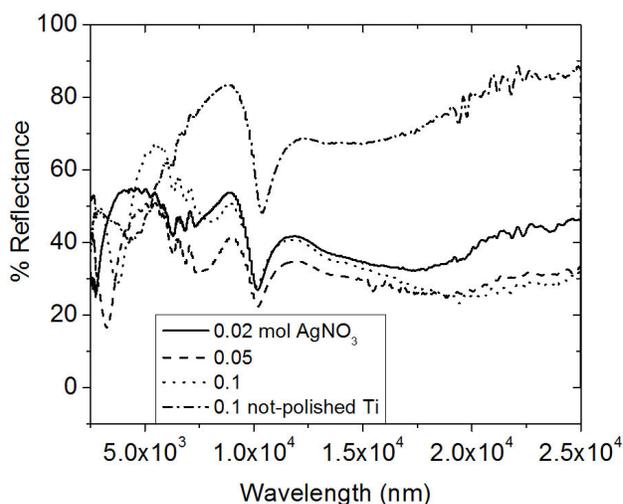

FIGURE 6. % Reflectance spectra for Al_2O_3-Ag Cermet coatings as a function of wavelength in the far infrared region of the electromagnetic spectrum.

4. Discussion

The reflections in the diffraction patterns are observed as wide peaks, indicating the nanostructured nature of Ag particles. There are no additional reflections in the diffraction patterns, suggesting that aluminum oxide does not manifest a crystalline structure. The amorphous phase of aluminum oxide is generally obtained by the ultrasonic spray pyrolysis technique even at temperatures as high as 650°C [25]. From the nanostructured characteristics of Ag particles, the crystallite size was estimated considering the reflection (111), making use of the Debye-Scherrer equation. The average value of the crystallite was about ∼17-26 nm. This result seems to confirm that the chemical reactions related to the decomposition of Al(acac)$_3$ and Ag(NO$_3$) are likely to be carried out simultaneously which favors the synthesis of Al$_2$O$_3$-Ag Cermets. In addition to this, it is highlighted the fact that the Cermet is obtained in nanostructured dimension. The AFM micrographs highlight the shape and distribution of the Ag nanoparticles in two selected Cermets. An estimate of the size of the Ag particles was done through a histograms analysis, which is displayed next to the SEM micrographs of Fig. 2. The statistical analysis shows that the average size of the particles and their standard deviations are the following: 9.4 ± 4.7 nm, 11.3 ± 5.14 nm, 27.1 ± 9.6 nm and 16 ± 3.4 nm, for those deposited with 0.01, 0.02, 0.05 and 0.1 mol of Ag(NO$_3$), respectively. It can be observed that the particle size is in the range obtained by XRD (Scherrer formula). The distribution of particles seems to be uniform and distributed over the entire surface, a situation that should be present to achieve the potential applications of the Cermets. The morphology and distribution of this type of Cermets is similar to the results reported in the literature that use Ag as a component in the Cermets [6,22]. In addition, it can be seen that as the content of Ag(NO$_3$) increases in the precursor solution, the particles tend to clump together in small clusters (Fig. 2d). This fact might probably impede a further growth of the Ag particles size when the Cermets are synthesized with 0.1 Mol of Ag(NO$_3$). However, a further work should be done with higher molarities to verify this hypothesis. It can be perceived that the increase in the content of Ag influenced strongly the optical absorption of the Cermet in the visible region, Fig. 3. It has been reported that the location and shape of the surface plasmon, due to Ag nanoparticles, depends on the shape of Ag nanoparticles. Other reports show the effect of different thermal treatments in the Cermets. For example, in the work of Yang *L et al.*, [22] the Ag particles, which result in 2.5 nm, reach an average value of 3.3 nm after a heat treatment at 200°C. Further annealing treatments carried out at 300°C and 400°C, resulted in Ag nanoparticles of 3.9 nm and 4.2 nm, respectively [22]. In this research, no annealing treatment was carried out after the Cermets deposition; these Cermets were characterized as deposited. However, the position of the plasmon resulted with a slight shift; showing the trend to move toward shorter wavelength as a function of the decrease in the Ag(NO$_3$) concentration in the deposition

solution. The results in Fig. 3 show that the plasmon was centered at 504 nm for deposited samples with 0.1 mol of Ag(NO$_3$), at 506 nm for deposited samples with 0.05 mol, at 497 nm for deposited samples with 0.02 mol and at 475 nm for deposited samples with 0.01 mol of Ag(NO$_3$) content. Barshilia *et al.* [1] found for the same Cermet, Al$_2$O$_3$-Ag, deposited by sputtering that the position of the plasmon is located at 610 nm, approximately. In the work of Yang Li, related to coatings of nano-composite of SiO$_2$-Ag, it is reported that the position of the peak has a blue-shift and the intensity of the peak decreases with the decrease in the size of the particles of Ag, probably by the non-homogeneity of the particles [22]. I.O. Sosa *et al.* reported that the excitation of the surface plasmon of Ag is located in the 350 nm and that its position depends strongly on the geometry of the Ag particles [30]. C. Noguez studied the influence of the shape and the physical environment in the surface plasmons on metal nanoparticles [31]. She showed that polyhedral nanoparticles with less faces showed more resonances and that in more symmetric nanoparticles the resonance was blue-shifted. Other effects were noticed when the nanoparticles were close to the substrate. Her work shows a dramatic influence of the shape and environment on the plasmon resonance [31]. It is observed in this work that the plasmon peak is shifted to longer wavelengths as the particle size increases, in agreement probably to previous reported results [32]. However, a further work should be done related to this issue since the location of the absorbance could also be due to possible changes in the particle shapes, their environment and/or to their closeness to the substrate [31]. In the best of cases, an absorptance and emittance of 0.83 and 0.14, respectively, were obtained for a sample of Al$_2$O$_3$-Ag deposited on a not polished titanium substrate. In this case, the Cermet was prepared with 0.1 mol of Ag(NO$_3$). Lower values, compared to the ones obtained in the literature, were found in this work, probably because our Cermets were characterized as they were deposited without any subsequent annealing treatment and/or any antireflective/anti-glare layer [1]. Further research is currently being undertaken with the purpose of being able to increase the selectivity in the studied Cermets in this contribution, in addition to the fact of considering different treatments on the metal surfaces for the possible applications as solar absorbing coatings. However, in this contribution it seems to be highlighted the feasibility of obtaining Al$_2$O$_3$-Ag Cermets by a simple route such as USP.

5. Conclusions

In summary, it is shown the feasibility for synthesizing Al$_2$O$_3$-Ag nano-Cermets coatings using the USP technique from Ag(NO$_3$) and Al(acac)$_3$ as sources of silver and aluminum, respectively. The XRD results confirmed emphatically the presence of metallic silver in the Cermets synthesized. The plasmon peak showed an increment in the corresponding absorption with the increase in the concentration of silver nitrate. The shape of the particles resulted mainly

spherical, with a size in the range from ∼9 nm to 27 nm, and their concentration was proportional to the concentration of $Ag(NO_3)$ in the deposition solution. By means of the UV-Vis, IR and FT-IR spectroscopies, it was determined, in the best of cases, an absorptance and an emittance of 0.83 and 0.14, respectively, for a sample of Al_2O_3-Ag prepared with 0.1 mol of $Ag(NO_3)$ in the precursor solution.

Acknowledgments

1. H.C. Barshilia, P. Kumar, K.S. Rajam and A. Biswas, *Solar Energy Materials & Solar Cells* **95** (2011) 1707-1715.

2. E. Barrera, T. Viveros, A. Montoya, and M. Ruiz, *Solar Energy Materials & Solar Cells* **57** (1999) 127-140.

3. C.G. Granqvist, *Appl. Phys. A* **52** (1991) 83-93.

4. H.G. Craighead, R. Bartynsky, R.A. Buhrman, L. Wojcik and A.J. Sievers, *Solar Energy Materials* **1** (1979) 105-124.

5. D.R. McKenzie *Appl. Phys. Lett.* **34** (1979) 25-28.

6. S.K. Mandal, R.K. Roy and A.K. Pal, *J. Phys. D: Appl. Phys.* **35** (2002) 2198-2205.

7. A. Chatterjee and D. Chakravorty, *J. Phys. D: Appl. Phys.* **22** (1989) 1386-1392.

8. R. Antoine *et al.*, *J. Appl. Phys.* **84** (1998) 4532-4536.

9. C.G. Granqvist and O. Hunderi, *J. Appl. Phys* **50** (1979) 1058-1065.

10. S. Cho, S. Lee, T.S. Lee, B.-k. Cheong, W.M. Kim and K.-S. Lee, *J. Appl. Phys.* **102** (2007) 123501.

11. J. Okumu, C. Dahmen, A.N. Sprafke, M. Luysberg, G.-V. Plessen and M. Wuttig, *J. Appl. Phys.* **97** (2005) 094305.

12. K. Zakrzewska, M. Radecka, A. Kruk, and W. Osuch, *Solid State Ionics* **157** (2003) 349-356.

13. S.K. Mandal, R.K. Roy, and A.K. Pal, *J. Phys. D: Appl. Phys.* **36** (2003) 261-265.

14. F. González, C.E. Barrera and C.R. Rosas, *Revista Mexicana de Ingeniería Química* **9** (2010) 79-83.

15. G.A. Niklasson and C.G. Granqvist, *Appl. Phys. Lett.* **41** (1982) 773-775.

16. G.A. Niklasson and C.G. Granqvist *J. Appl. Phys.* **55** (1984) 3382-3410.

17. J. Blain, C. LeBel, R.G. SaintJacques, and F. Rheault, *J. Appl. Phys.* **5** (1985) 490-494.

18. A. Andersson, O. Hunderi, and G.C. Granqvist, *J. Appl. Phys.* **51** (1980) 754-764.

19. G. Blandenet, M. Court, and Y. Lagarde, *Thin Solid Films* **77** (1981) 81-90.

20. M. Langlet and J.C. Joubert *The pyrosol process or the pyrolysis of an ultrasonically generated aerosol. In: Rao CNR* (ed.) Chemistry of Advanced Materials. Blackwell Scientific Publications, Oxford (1993). pp. 55-79.

21. T.T. Kodas and M.J. Hampden-Smith, *Aerosol Processing of Materials*, (Wiley-VCH 1999).

22. L. Yang, G.H. Li and L.D Zhang, *Appl. Phys. Lett.* **76** (2000) 1537-1539.

23. H.G. Craighead, R.E. Howard, and J.E. Sweeney, *Appl. Phys. Lett.* **39** (1981) 29-31.

24. G.A. Nyberg and R.A. Buhrman *Appl. Phys. Lett.* **40** (1982) 129-131.

25. M. Aguilar-Frutis, M. Garcia, and C. Falcony, *Appl. Phys. Lett.* **72** (1998) 1700-1702.

26. M. Aguilar-Frutis, M. Garcia, C. Falcony, G. Plesch and S. Jimenez-Sandoval, *Thin Solid Films* **389** (2001) 200-206.

27. S. Carmona-Tellez *et al.*, *J. Appl. Phys.* (2008) 103-034105.

28. A. Politycki and K. Hieber, *Deposition of metal, carbide and oxide films by thermal decomposition of metal acetylacetonates*, In: Chapman BN and Anderson JC (eds) Science and Technology of Surface Coatings. London, Academic Press, (1974) pp. 159-168.

29. R.I. Sánchez-Alarcón *et al.*, *J. Phys. D: Appl. Phys.* **49** (2016) 175102.

30. I.O. Sosa, C. Noguez and R.G. Barrera, *J. Phys. Chem. B* **107** (2003) 6269-6275.

31. C. Noguez, *J. Phys. Chem. C* **111** (2007) 3806-3819.

32. O. Stenzel, *The Physics of Thin Film Optical Spectra, An Introduction*, Springer-Verlag Berlin Heidelberg (2005).